Conf-920673--10

PNL-SA--19945

DE92 019372

Isotopic Tailoring with ^{59}Ni to Study the Effect of Helium on Microstructural Evolution and Mechanical Properties of Neutron-Irradiated Fe-Cr-Ni Alloys

F. A. Garner
M. L. Hamilton
L. R. Greenwood
J. F. Stubbins[a]
B. M. Oliver[b]

March 1992

16th International Symposium
on Effects of Radiation on Materials
Denver, Co.
June 20-24, 1992

Work supported by
the U.S. Department of Energy
under Contract DE-AC06-76RLO 1830

Pacific Northwest Laboratory
Richland, Washington 99352

(a) University of Illinois
Urbana, IL 61801
(b) Rockwell International
Canoga Park, CA 91303

Introduction

Until recently it has been impossible to conduct experiments in which spectrum-related parameters such as helium/dpa ratio were varied without also accepting variations in other important parameters such as displacement rate or temperature history. A technique currently being used, however, allows the study of the influence of helium alone on density change, microstructural evolution, and mechanical properties. This technique utilizes isotopic tailoring to vary the helium production rate without introducing changes in neutron spectrum or displacement rate.[1,2] By producing alloys whose only difference is the presence or absence of ^{59}Ni, an isotope that does not occur naturally, and irradiating doped and undoped specimens side-by-side in the appropriate reactor spectra, it is possible to generate substantial variations in He/dpa ratio without varying any other important parameter. The ^{59}Ni isotope produces helium by an (n, α) reaction whose cross section increases with decreasing neutron energy.[3]

A particular advantage of comparative isotopic doping experiments is that one need not be concerned with the details of temperature history, which are now known to heavily influence the outcome of some fission-fusion correlation experiments.[4,5] Because both doped and undoped specimens are irradiated side-by-side, the primary variable is only the helium/dpa ratio. The production rate of helium in doped specimens is also nearly, but not exactly, constant throughout the experiment, providing that no changes occur in the neutron environment.[6]

This report presents a compilation of all tensile data and some of the

recent microstructural data obtained from the ^{59}Ni isotopic doping experiment conducted in the Materials Open Test Assembly (MOTA) of the Fast Flux Test Facility (FFTF). The results of post-irradiation helium measurements are also presented and evaluated to determine the factors that influence the conduct and interpretation of isotopic doping experiments.

Experimental Details

The alloys employed in this study were nominally Fe-15Cr-25Ni, Fe-15Cr-25Ni-0.04P and Fe-15Cr-45Ni (wt%) in both the cold worked and annealed conditions. These alloys were chosen to complement those used in several earlier studies, one in the Experimental Breeder Reactor-II (EBR-II), designated the AD-1 experiment,[7,8] and another conducted in the Oak Ridge Research (ORR) Reactor, designated MFE-4.[8] The acquisition of the ^{59}Ni, the production of the ^{59}Ni-doped tensile specimens, and their irradiation conditions are described in Reference 1. Microscopy disks were also prepared and irradiated; the results of examination of the first several discharges of these specimens are described in detail in References 9 to 11. The miniature tensile specimens measured 5.1 mm, 1.0 mm, and 0.25 mm in gauge length, width, and thickness, respectively. They were tested at room temperature at a strain rate of 4.7×10^{-4} sec^{-1} in a horizontal test frame described in Reference 12. Yield strengths were determined at 0.2% offset. In some cases, more than one tensile specimen was tested, but the majority of tests to date have involved only a single test specimen. Some of the early results of these experiments were presented in other papers.[13,14]

Results of Tensile Tests

Figure 1 provides a schematic representation of the various irradiation sequences of the ^{59}Ni experiment, each sequence defined by its target irradiation temperature and location in FFTF-MOTA. The experiment was initiated in MOTA 1D, but a short (~50 minutes) temperature excursion in FFTF Cycle 7, referred to as an overtemperature event, compromised the integrity of many of the experiments in the MOTA. A decision was made, therefore, to run the MOTA in the helium-purged mode for the remainder of FFTF Cycles 7 and 8 while a series of reactivity feedback tests were conducted. The majority of the MOTA canisters therefore operated at variable but lower-than-target temperatures until the end of Cycle 8. Isothermal irradiation then proceeded in MOTA 1E, 1F, and 1G.

The original 600°C sequence was not continued to higher exposure due to the magnitude of the temperature excursion, which reached 806°C for fifty minutes. The 495°C sequence reached 629°C for fifty minutes, but was continued in MOTA-1E along with a replacement sequence of duplicate specimens at 495°C to evaluate the effect of temperature history. A similar replacement was made for the sequence at 490°C, although the original sequence was not continued. The sequences at 365°C and 465°C did not experience significant temperature excursions during MOTA 1D and were continued without replacement. Both the 465 and 490°C above-core sequences experienced lower-than-target temperatures during Cycle 8, but the magnitude of the average temperature decrease was not as pronounced as that at 495°C.

Three tensile tests on unirradiated specimens were conducted for each undoped alloy in both the cold worked and the annealed conditions. Since the availability of doped specimens was rather limited, only one doped specimen was tested for each combination of alloy and thermomechanical starting condition. Figure 2 shows that the range of yield strengths in the undoped specimens is not large and that the single doped specimen in each condition did not exhibit any significant difference in behavior. Also shown in Figure 2 are the yield strengths exhibited by the larger specimens of the unirradiated annealed alloys that were irradiated in the AD-1 and MFE-4 experiment. [8] This comparison demonstrates the excellent agreement among the three experiments and indicates an independence on specimen size of the results [15].

Figures 3-7 show the yield strength and elongation data of irradiated specimens measured at room temperature. The width of the error bars at zero dpa on the yield stress plots corresponds to the variation seen in Figure 2 for unirradiated specimens and provides a basis for determining whether variations observed between doped and undoped specimens after irradiation are significant compared to the scatter associated with the measurement technique. Similar error bars are shown for the elongation data.

The most significant features of the data shown in these figures are, first, the relative unimportance of the helium generation rate at all temperatures studied in determining the tensile properties, and second, the convergence of the tensile properties of both annealed and cold worked specimens to levels that depend only on irradiation temperature. A similar

convergence was observed earlier in 316 stainless steel over a wide range of irradiation temperatures, with convergence levels sensitive to both temperature and displacement rate.[16-18]

At 495°C only annealed tensile specimens were irradiated and therefore it is not possible to determine whether convergence occurs at this temperature. However, transmission electron microscopy (TEM) disks were irradiated at 495°C in both the annealed and cold worked conditions and convergent microstructures appear to have developed in specimens irradiated to 14 dpa.[9] The tensile data at 495°C also demonstrate another type of convergence. Note that the strength of the original specimens (i.e., those subjected to the overtemperature and subsequent low temperature irradiation) initially reached a very high level and then fell to lower levels during the second and third irradiation sequences. The specimens in the replacement sequence reached the same lower levels directly, however. Similar but inverted behavior is evident in the elongation data. The specimens exhibited lower ductility levels initially, followed by higher ductility levels when the originally intended irradiation temperature (495°) was reestablished. Thus, both the microstructure and tensile properties converge at levels dependent more on the recent irradiation temperature history rather than on the earlier temperature history.

The tendency for the temperature history to produce differences in strength appears to be related to the composition of the alloy, however. Note that in both the 495 and 490°C sequences that the tensile properties of the 25Ni alloy was more susceptible to temperature history than that of the other

two alloys.

The high strength levels that were reached in the first irradiation interval of the 495 and 490°C sequences did not arise from the temperature excursion itself, but from the prolonged irradiation at lower temperatures that followed the overtemperature event. The higher density of microstructure and the resulting higher strength and lower ductility that developed at the lower temperatures were replaced later by microstructures and tensile properties more appropriate to the temperatures achieved in the second and third irradiation segments. The persistent influence of temperature history observed by Kiritani et al.[4] in low fluence irradiations did not occur in this higher fluence experiment.

The tensile properties of each of the three alloys have definitely converged at 365°C, both as a function of starting state and helium/dpa level. Since the difference between the helium generation rates was large in the 365°C series, and relatively large dpa levels were also attained, the microstructures of the 365°C specimens were investigated at the 10.3 dpa level to determine the microstructural origin of the convergence.[11] As shown in Figure 8, high helium levels increased the void density in general, but this was usually compensated by a reduction in void size. The swelling levels are rather small in each case and no consistent influence of helium on the total swelling was found. Using standard models for hardening by each microstructural component,[16] a comparison was made of the predicted vs. measured yield strengths[11] as shown in Figure 9. It appears that the convergence in strength is mirrored in the convergence of microstructure.

Neither the starting state nor the helium level influence the saturation strength level to any significant degree.

Results of Helium Measurements

The post-irradiation helium levels were recently measured using standard techniques, [19,20] at Rockwell International on cold worked Fe-15Cr-25Ni specimens from all irradiation temperatures in the second and third discharges of the experiment and on cold worked Fe-15Cr-45Ni specimens at 365 and 490°C in the second discharge. Helium measurements for the first discharge were reported in Ref. 13. Helium production was not measured in the Fe-15Cr-45Ni alloy for the first discharge; instead, helium levels for Fe-15Cr-45Ni in the first discharge were calculated from composition ratios and measurements made on Fe-15Cr-25Ni.

Tables 1-3 present the helium concentrations obtained on two samples cut from each specimen from the second and third discharges of the ^{59}Ni doping experiments. Note that the measurements made on specimens removed from three of the second discharge groups (at 365, 495 and 465°C) and both of the third discharge groups [495°C(R) and 490°C(R)] represent the average helium levels for irradiation during two MOTA irradiation cycles (1D and 1E or 1E and 1F). Because the first and second sets of specimens discharged at each temperature were originally irradiated side-by-side it is possible to calculate the average helium formation rate that occurred in the second MOTA irradiation cycle only. These values are shown in parentheses in Table 2.

As shown in Table 2, the helium generation rates in both undoped and doped Fe-15Cr-25Ni specimens at 365°C (below the core) increased substantially in MOTA 1E compared to the rates observed in MOTA 1D. No change in position occurred between the two irradiation cycles, although some changes were made in the surrounding experiments. The average helium generation rates observed in Fe-15Cr-25Ni and Fe-15Cr-45Ni after the second discharge at 365°C exhibited the expected dependence on nickel content, (1.24 and 16.5 appm/dpa predicted vs. 1.20 and 16.7 measured for Fe-15Cr-45Ni) which confirms the validity of helium/dpa ratios calculated previously for Fe-15Cr-45Ni in the first discharge. As demonstrated later, however, this conclusion applies only to situations where the 25Ni and 45Ni specimens remain closely side-by-side throughout the full irradiation sequence.

In the original 495°C irradiation sequence in level 1, smaller but significant increases in helium generation rates were observed in both undoped and doped specimens relative to the increases observed at 365°C below core. These specimens were moved from the 1D4 position in MOTA 1D to the 1A4 position in MOTA 1E with no significant consequence on the helium production rate of the undoped specimens.

The replacement irradiation sequence at 495°C started in position 1A4 in MOTA 1E, along with the second irradiation cycle of the original 495°C series, and continued in position 1C3 in MOTA 1F. In the undoped replacement specimen, cumulative helium/dpa ratios of 0.44 and 0.57 appm/dpa were reached in the first and second irradiation sequences. These are higher than the 0.35 (position 1D4) and 0.47 values (positions 1D4 and then 1A4) reached in the

original series. This implies that in level 1 some spectral variation occurred between 1D4 of MOTA 1D and 1C3 of MOTA 1F. When the 495°C replacement series was moved to position 1C3 in MOTA 1F for its second irradiation cycle, this caused a substantial decrease in the helium production rate for the doped specimens. This probably reflects changes in the spectrum due to neighboring experiments. The production rate for the undoped specimens increased, reflecting the continued buildup of ^{59}Ni, a process that would continue to some degree for undoped specimens in all reactor positions.

In the 490°C replacement sequence, the helium production rate rose between MOTA 1E and MOTA 1F for both the undoped and doped specimens. No change in position occurred during this irradiation sequence. Both the original and replacement sequences proceeded in position 6E2, which is an above-core position possessing a large axial gradient in neutron flux and apparently significant changes in the details of the spectrum that affect the burnout and production of ^{59}Ni.

Several consequences of such changes in the neutron environment can be seen in the two irradiation sequences at 490°C. First, the helium/dpa ratios for both specimen types in the replacement sequence are somewhat lower than that of the original sequence, probably reflecting differences in the loading of nearby components during the operation of MOTA 1D and MOTA 1E. Second, based on the measured MOTA-1E production rates in undoped Fe-15Cr-25Ni, we would expect the production rate in undoped Fe-15Cr-45Ni to be 0.38 appm/dpa, whereas only 0.30 appm/dpa was measured. The difference between helium levels in the 25Ni and 45Ni doped specimens is also somewhat larger than expected.

These observations imply that the 45Ni specimens, which were in a separate packet from the 25Ni specimens, experienced a slightly different spectral environment, even though they were in the same MOTA basket. This in turn suggests that significant radial gradients in spectral parameters must also exist and that the specimens may not have been irradiated closely side-by-side.

The 465°C low fluence sequence was conducted in above core position 8F1 in both MOTA 1D and MOTA 1E. In this case, the production rates of both the doped and undoped specimens increased. Note that the production rates in the doped specimens are quite large, 54 and 71 appm/dpa in Fe-15Cr-25Ni in MOTA 1D and MOTA 1E, respectively.

Review of the data in Tables 1 and 2 leads to the following generalizations: 1) helium production in undoped specimens containing only natural nickel is greatest for irradiation within the core; 2) significant increases in helium production rate occur with increasing exposure in undoped specimens regardless of location with respect to the core. The percentage increases are greatest for irradiations conducted outside the core. 3) helium production rates in specimens doped with ^{59}Ni before irradiation tend to increase also, but are much more sensitive to changes in neutron spectrum arising from changes in position or changes in neighboring components. In some cases, the helium production rate of doped specimens can actually decrease, even though undoped specimens in the same reactor position experience increases in helium production. This difference is due to the fact that ^{59}Ni production varies roughly as the second power of the dpa level,

while the burn-out of ^{59}Ni is roughly linear with dpa.[21] Both reactions are separately but strongly sensitive to fine details of the neutron spectra.

Note that the various irradiation sequences were all conducted near or outside the edges of the FFTF core. Since the cross sections for production of ^{59}Ni from ^{58}Ni and the production of helium from ^{59}Ni depend not only on the neutron fluence but also strongly on the neutron spectrum, the helium production rate is strongly dependent on location,[6] peaking outside the core as shown in recent idealized calculations, Figure 10. Since the dpa rate falls while the helium production rate per neutron increases, the helium/dpa ratio peaks even more strongly, as shown in Figure 11. Thus, near-edge core positions produce the optimum combination of helium/dpa ratio and dpa level. It should be noted, however, that the calculated helium/dpa ratio shown in Figure 11 peaks at lower values than actually measured (~20 vs. ~60), reflecting the uncertainties in flux and spectra discussed in the previous paragraph. This discrepancy highlights the need for actual helium measurements in order to conduct these experiments successfully.

Conclusions

Doping nickel-containing austenitic model alloys with the ^{59}Ni isotope and irradiating side-by-side with undoped specimens in the appropriate near-edge regions of the FFTF core produces a successful one-variable experiment directed toward the influence of helium on radiation-induced microstructural development and the resultant changes in mechanical properties. Because the cross sections for burn-in and burn-out of ^{59}Ni are very sensitive to local

variations in neutron spectra, and the production of ^{59}Ni is nonlinear with neutron fluence, post-irradiation measurements of helium concentrations are necessary for the successful conduct of such experiments, especially in the out-of-core regions.

When model Fe-Cr-Ni alloys are irradiated at a constant displacement rate, but at very different helium/dpa ratios in the range 365 to 600°C, there is no significant variation in their tensile properties as a function of helium. A similar conclusion was reached by Mansur and Grossbeck [22] in a comparison of data from EBR-II and the High Flux Isotope Reactor on the Japanese and U.S. versions of PCA, the Prime Candidate Alloy of the fusion materials program. Although the displacement rates in those two reactors were comparable, the differences in helium generation rates in that comparison were even larger than in the current experiment. In the absence of variations in displacement rate, the impact of high helium generation appears to be small and secondary to the influence of cold work, temperature, nickel level, and phosphorus level. It appears that tensile properties converge to a saturation level that depends primarily on alloy composition and recent irradiation temperature, but not on early temperature history or helium generation rate. This convergence is a result of microstructures which also converge.

REFERENCES

[1] R. L. Simons, H. R. Brager and W. Y. Matsumoto, J. Nucl. Mater. 141-143 (1986) 1057-1060.

[2] G. R. Odette, J. Nucl. Mater. 141-143 (1986) 1011-1017.

[3] Ch. De Raedt, in Proc. Conf. on Fast, Thermal, and Fusion Reactor Experiments, April 1982, Salt Lake City (American Nuclear Society, La Grange Park, IL, 1982) p. 226.

[4] M. Kiritani, J. Nucl. Mater. 160 (1988) 135-141.

[5] N. Sekimura, F. A. Garner and R. D. Griffin, J. Nucl. Mater. in press.

[6] L. R. Greenwood, F. A. Garner and B. M. Oliver, J. Nucl. Mater. in press.

[7] H. R. Brager, F. A. Garner and M. L. Hamilton, J. Nucl. Mater. 133 & 134 (1985) 594-598.

[8] M. L. Hamilton, A. Okada and F. A. Garner, J. Nucl. Mater. 179-181 (1991) 558-562.

[9] J. F. Stubbins and F. A. Garner, J. Nucl. Mater. 179-181 (1991) 573-575.

[10] H. Kawanishi, F. A. Garner and R. L. Simons, J. Nucl. Mater. 179-181 (1991) 511-514.

[11] J. F. Stubbins and F. A. Garner, J. Nucl. Mater. in press.

[12] N. F. Panayotou, S. D. Atkin, R. J. Puigh and B. A. Chin, The Use of Small-Scale Specimens for Testing Irradiated Material, ASTM STP 888, W. R. Corwin and G. E. Lucas, Eds., American Society for Testing and Materials, Philadelphia, 1986, pp. 210-219.

[13] F. A. Garner, M. L. Hamilton, R. L. Simons and M. K. Maxon, J. Nucl. Mater. 179-181 (1991) 554-557.

[14] M. L. Hamilton and F. A. Garner, J. Nucl. Mater. (in press).

[15] F. A. Garner, M. L. Hamilton, H. L. Heinisch and A. S. Kumar in Proceedings, ASTM International Symposium on Small Specimen Test Techniques and Their Applications to Pressure Vessel Annealing and Plant Life Extension (in press).

[16] F. A. Garner, M. L. Hamilton, N. F. Panayotou and G. D. Johnson, J. Nucl. Mater. 103 & 104 (1981) 803-808.

[17] F. A. Garner, H. L. Heinisch, R. L. Simons and F. M. Mann, Radiation Effects and Defects in Solids 113 (1990) 229-255.

[18] H. R. Brager, L. D. Blackburn and D. L. Greenslade, J. Nucl. Mater. 122 & 123 (1984) 332.

[19] H. Farrar IV and B. M. Oliver, J. Vac. Sci. Technol. A4, (1986), 1740.

[20] B. M. Oliver, J. G. Bradley, and H. Farrar IV, Geochim. Cosmochim. Acta 48, (1984), 1759.

[21] L. R. Greenwood, J. Nucl. Mater. 115 (1983) 137.

[22] L. K. Mansur and M. L. Grossbeck, J. Nucl. Mater. 155-157 (1988) 130-147.

Table 1
Helium Concentrations Measured in Cold Worked TEM Disks

Temperature (°C)	Nickel (wt%)	Doped with ^{59}Ni	dpa	Specimen Mass[a] (mg)	^{4}He Measured (10^{14} atoms)	Helium Concentration (appm)[b] Measured	Helium Concentration (appm)[b] Average[c]
365	25	No	10.3	1.937	1.493	7.157	7.12
				2.966	2.263	7.084	±0.05
365	25	Yes	10.3	2.744	48.86	165.3	165
				3.186	56.34	164.2	±1
365	45	No	10.3	2.562	3.375	12.35	12.4
				3.024	4.015	12.44	±0.1
365	45	Yes	10.3	1.966	36.48	171.3	172
				3.339	61.24	171.9	±1
495	25	No	28.9	1.733	2.546	13.64	13.7
				3.410	5.016	13.66	±0.1
495	25	Yes	28.9	2.482	36.22	135.5	136
				3.316	48.46	135.7	±1
495(R)[d]	25	No	14.7	2.644	1.834	6.441	6.50
				3.374	2.385	6.563	±0.09
495(R)	25	Yes	14.7	3.174	23.82	69.68	69.2
				3.554	26.28	68.66	±0.7
495(R)	25	No	29.4	2.087	3.797	16.89	16.8
				2.360	4.247	16.71	±0.1
495(R)	25	Yes	29.4	2.826	36.49	119.9	120
				2.983	38.66	120.3	±1
490(R)	25	No	2.13	2.881	0.1383	0.4457	0.440
				4.212	0.1974	0.4352	±0.007
490(R)	25	Yes	2.13	2.861	6.691	21.71	21.5
				3.643	8.386	21.37	±0.2
490(R)	45	No	2.13	2.709	0.1865	0.6452	0.640
				3.241	0.2197	0.6353	±0.007
490(R)	45	Yes	2.13	2.785	7.296	24.55	24.1
				3.555	8.959	23.62	±0.7
490(R)	25	No	4.15	2.348	0.3590	1.420	1.42
				3.797	0.5808	1.420	±0.00
490(R)	25	Yes	4.15	2.735	16.87	57.27	56.8
				3.177	19.28	56.35	±0.7
465	25	No	0.28	2.825	0.02223	0.07306	0.0727
				3.129	0.02438	0.07235	±0.0005
465	25	Yes	0.28	2.780	5.201	17.37	17.4
				2.746	5.134	17.36	±0.1

(a) Mass uncertainty is ±0.001 mg. Two samples were cut from each original TEM specimen.
(b) Measured helium concentration in atomic parts per million (10^{-6} atom fraction) with respect to the calculated number of atoms in the specimen.
(c) Mean and 1σ standard deviation of duplicate analyses.
(d) R denotes replacement series.

Table 2
Helium Generation Rates Determined in Fe-15Cr-25Ni

Temperature (°C)	Helium Generation Rate (apprn/dpa)					
	MOTA 1D		MOTA 1E		MOTA 1F	
	Undoped	Doped	Undoped	Doped	Undoped	Doped
365	0.30	13.9	0.69[a] (1.26)[b]	16.0[a] (19.1)	No Discharge	
495	0.35	4.69	0.47[a] (0.59)	4.71[a] (4.73)	No Discharge	
495(R)[c]	Not Irradiated		0.44	4.71	0.57[a] (0.70)	4.08[a] (3.45)
600	0.40	4.4	Not Irradiated		Not Irradiated	
490	0.28	19.8	Not Irradiated		Not Irradiated	
490(R)[c]	Not Irradiated		0.21	10.1	0.34[a] (0.46)	13.7[a] (17.2)
465	0.14	54.3	0.26[a] (0.40)	62.1[a] (71.1)	No Discharge	

[a] He/dpa level given is the average for a two-cycle irradiation sequence.
[b] Helium/dpa levels in parentheses represent average values calculated for the second MOTA cycle only.
[c] R denotes replacement series.

Table 3
Cumulative Helium Generation Rates Determined in Fe-15Cr-45Ni After Discharge from MOTA-1E

Temperature (°C)	appm/dpa		Neutron damage (dpa)		
	Undoped	Doped	MOTA-1D	MOTA-1E	Total
365	1.20	16.7	6.1	4.2	10.3
490(R)	0.30	11.3	0.0	2.13	2.13

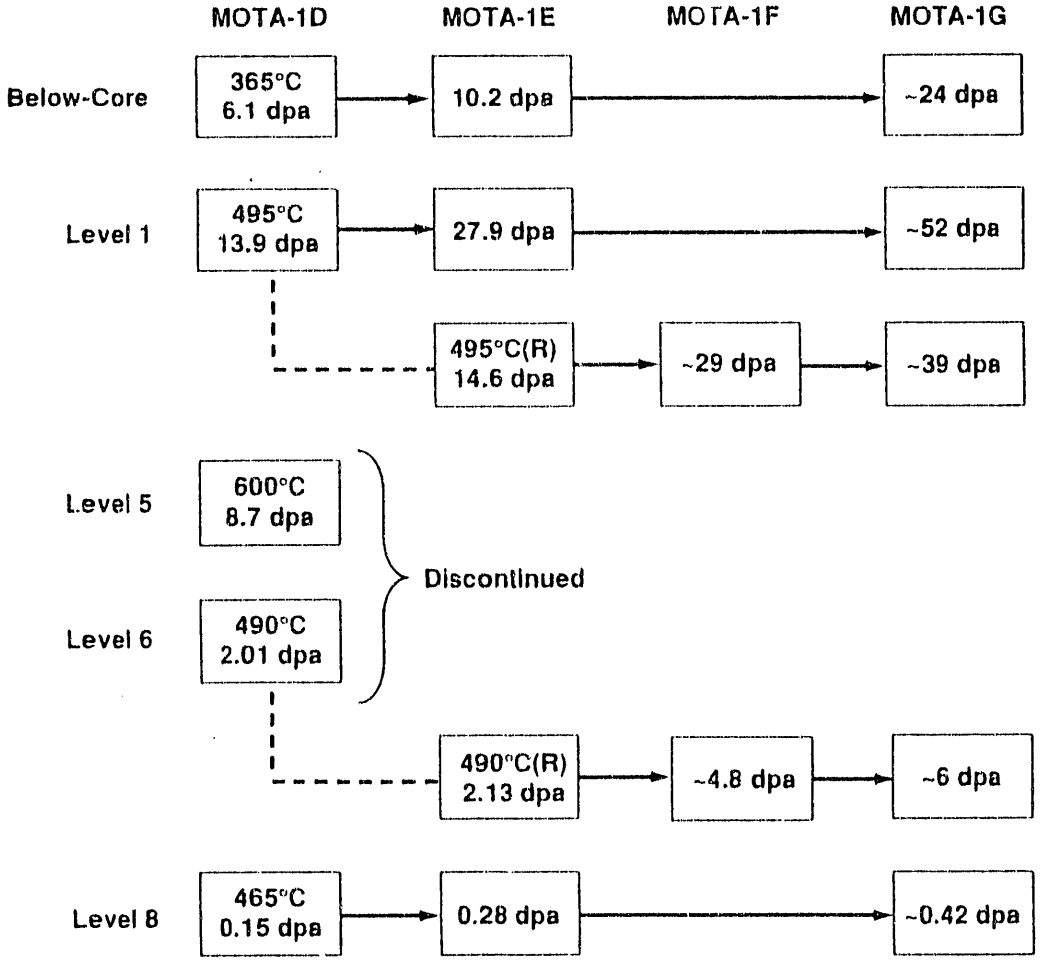

FIG. 1-- Schematic representation of irradiation sequences for the ^{59}Ni isotopic tailoring experiment. "495°C(R)" and "490°C(R)" refer to the replacement sequences substituted for the original compromised sequences at 495 and 490°C. Damage levels shown represent cumulative totals.

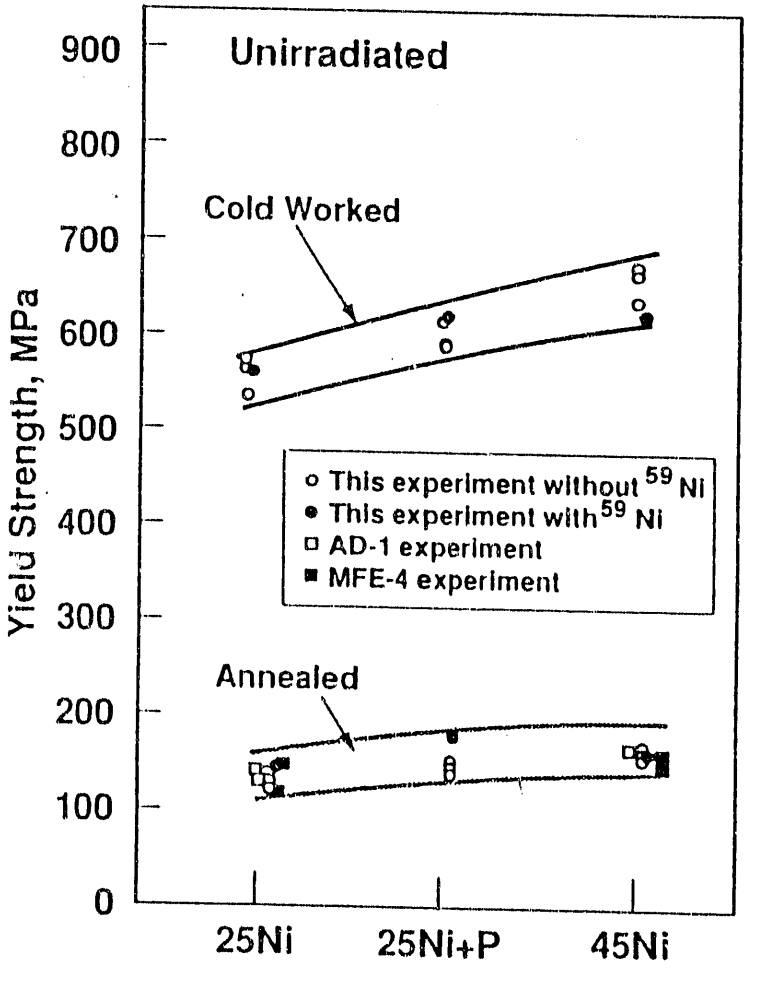

FIG. 2--Yield strength data on unirradiated specimens from the FFTF/MOTA ^{59}Ni experiment and two related experiments conducted in other reactors.

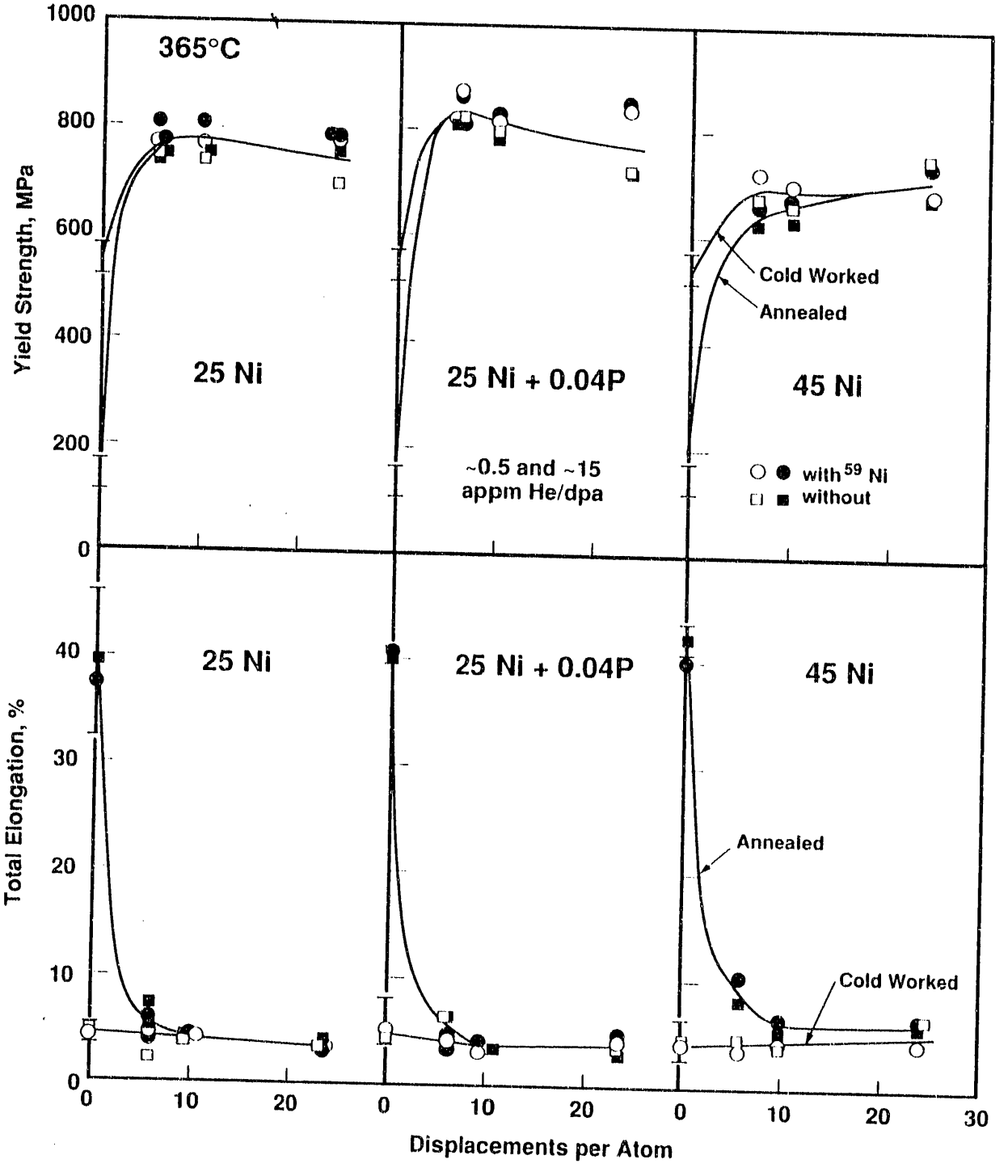

FIG. 3--Influence of thermomechanical starting state and isotopic doping on yield strength and elongation of three alloys irradiated below the core at 365°C. Filled and open symbols denote annealed and cold worked specimens, respectively, in this and the following figures. The average helium generation rates for undoped and doped specimens in the first two irradiation sequences are shown on each figure.

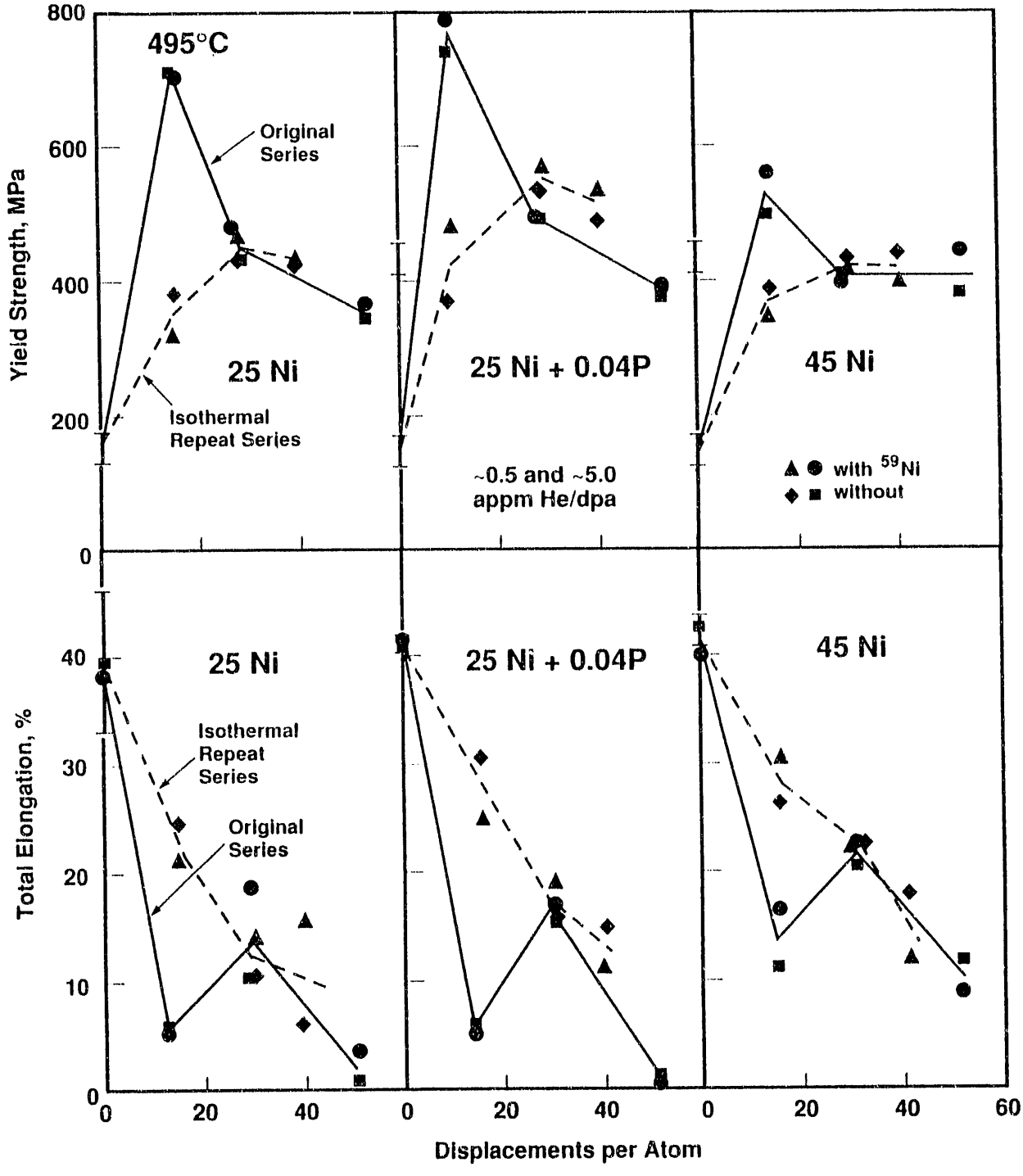

FIG. 4--Influence of isotopic doping and temperature history on the yield strength and elongation of annealed alloys following irradiation at the bottom of the core at 495°C. The dotted line corresponds to the isothermal repeat sequence.

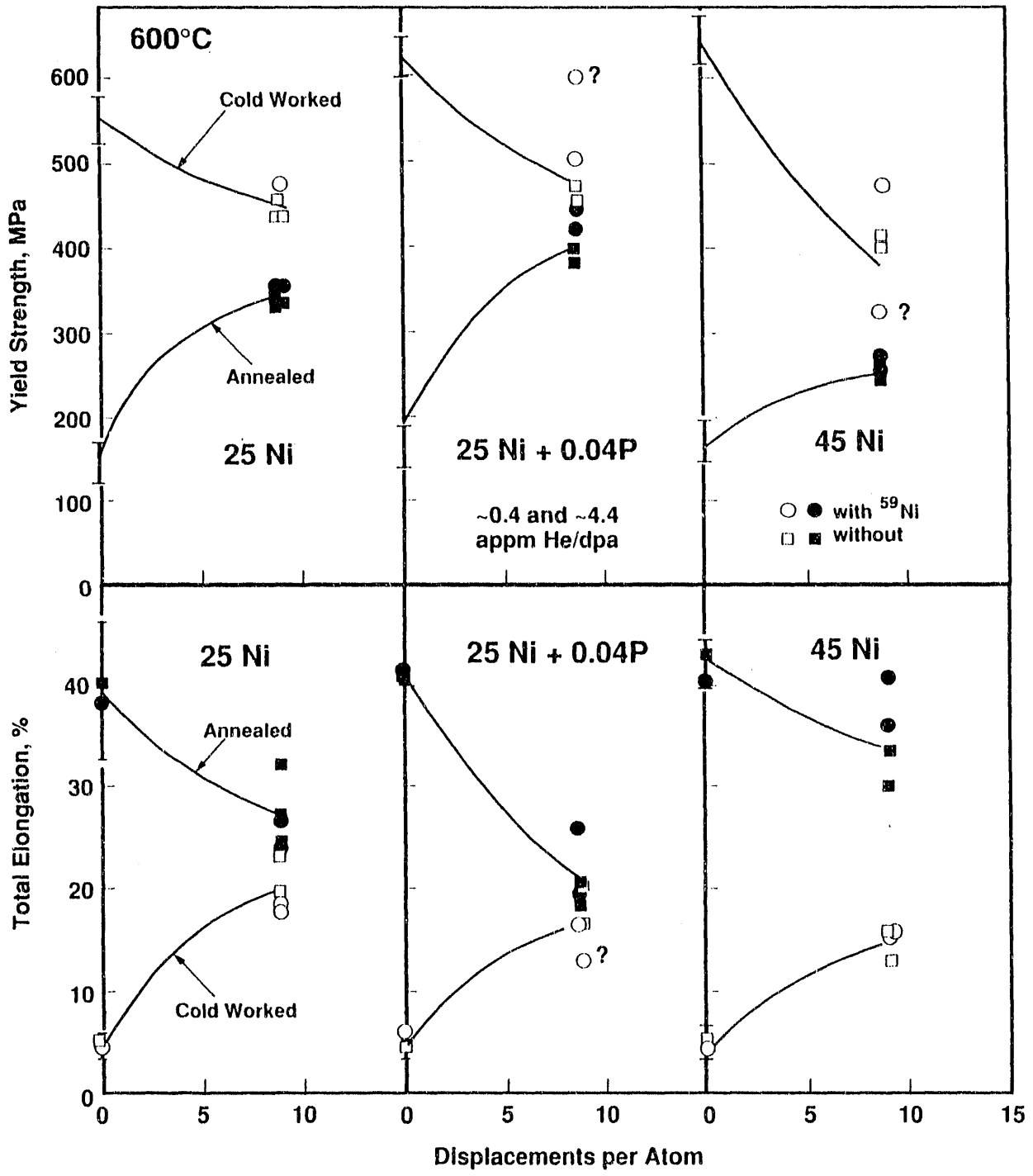

FIG. 5--Influence of isotopic doping and thermomechanical starting state on yield strength and elongation following irradiation at the top of the core at 600°C. This experiment was not continued beyond the first irradiation sequence.

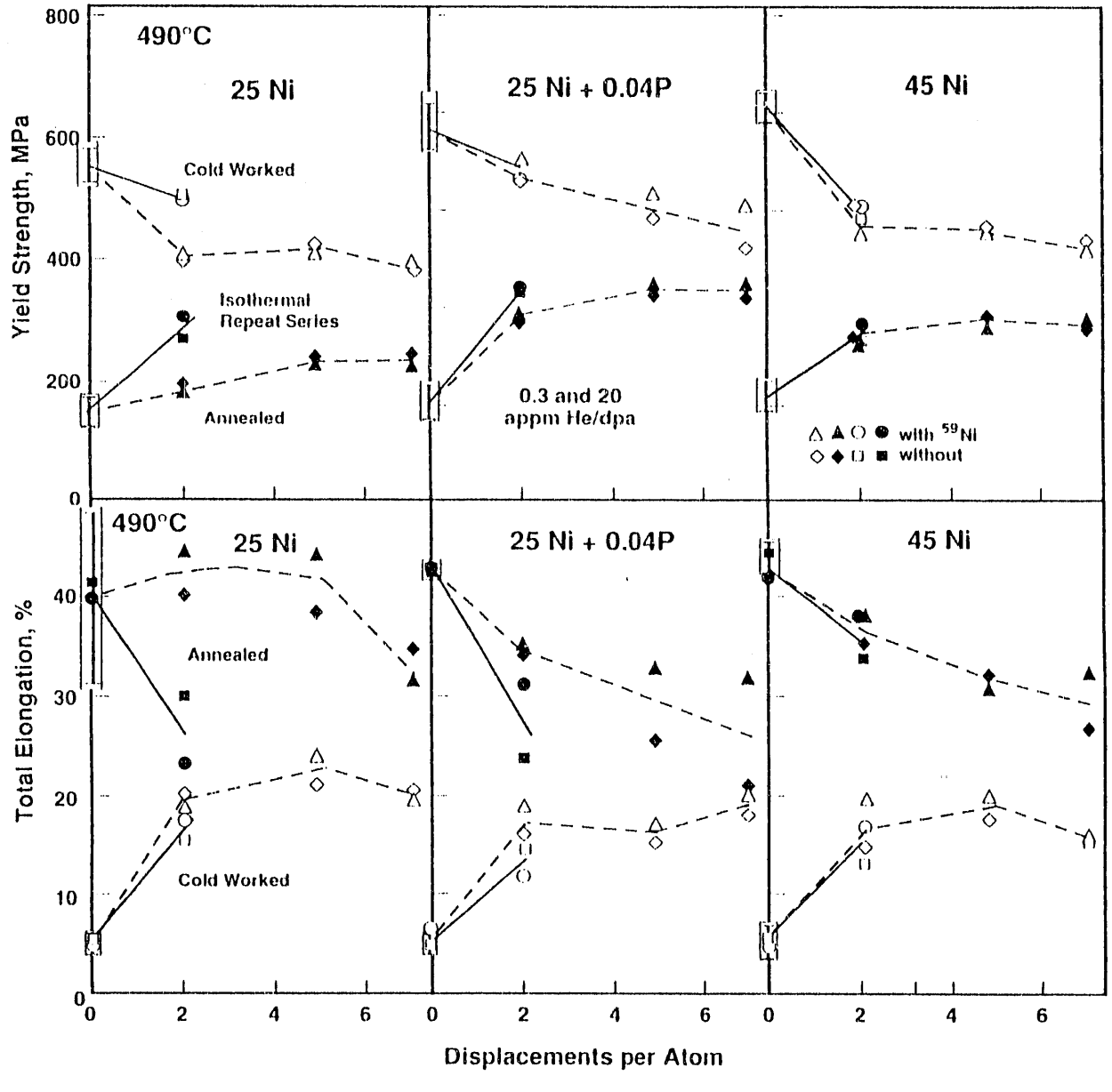

FIG. 6--Influence of thermomechanical starting state, isotopic doping and temperature history on yield strength and elongation following irradiation above the core at 490°C. The dotted lines correspond to the isothermal repeat sequence.

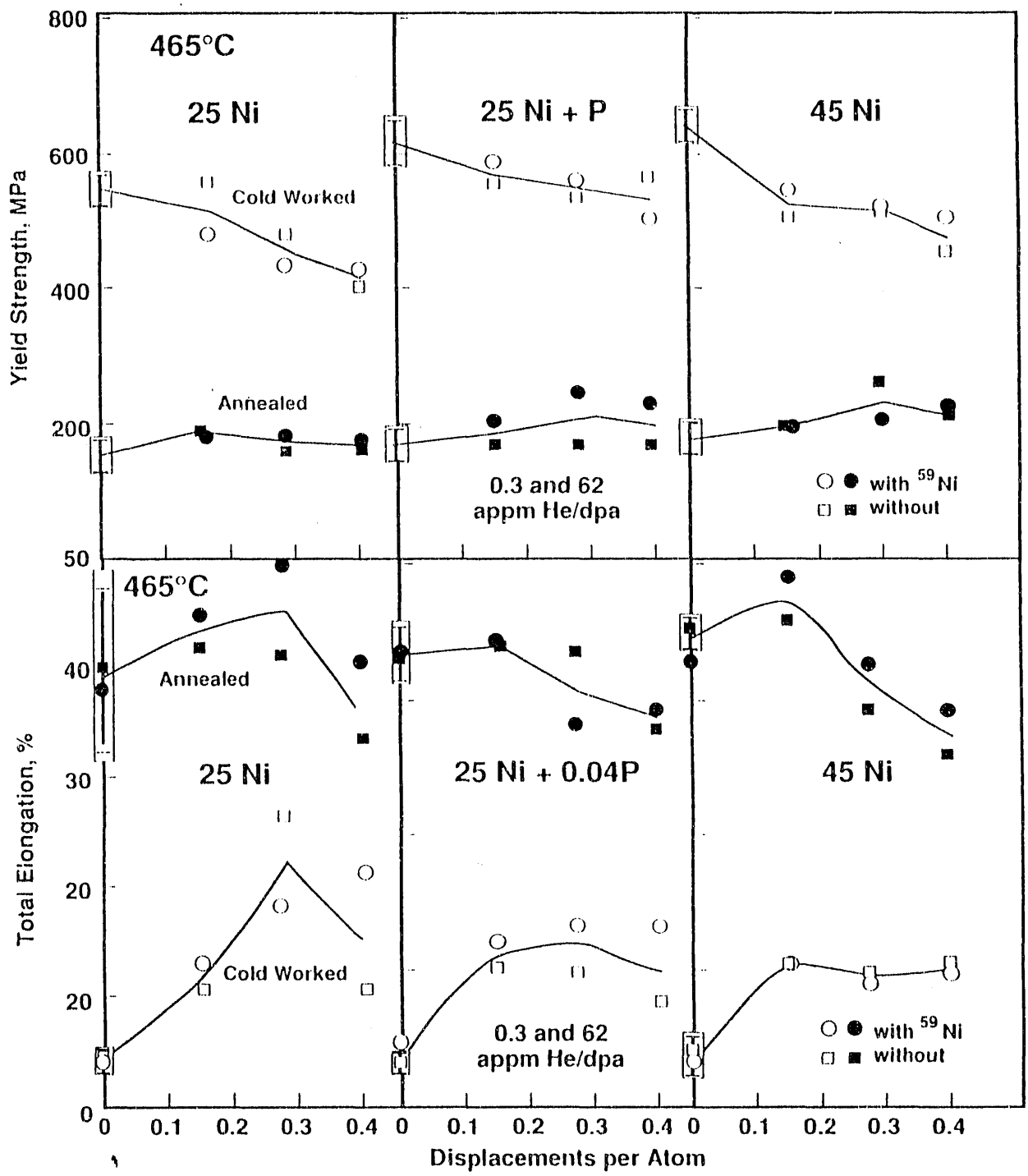

FIG. 7--Influence of thermomechanical starting state and isotopic doping on yield strength and elongation following irradiation above the core at 465°C.

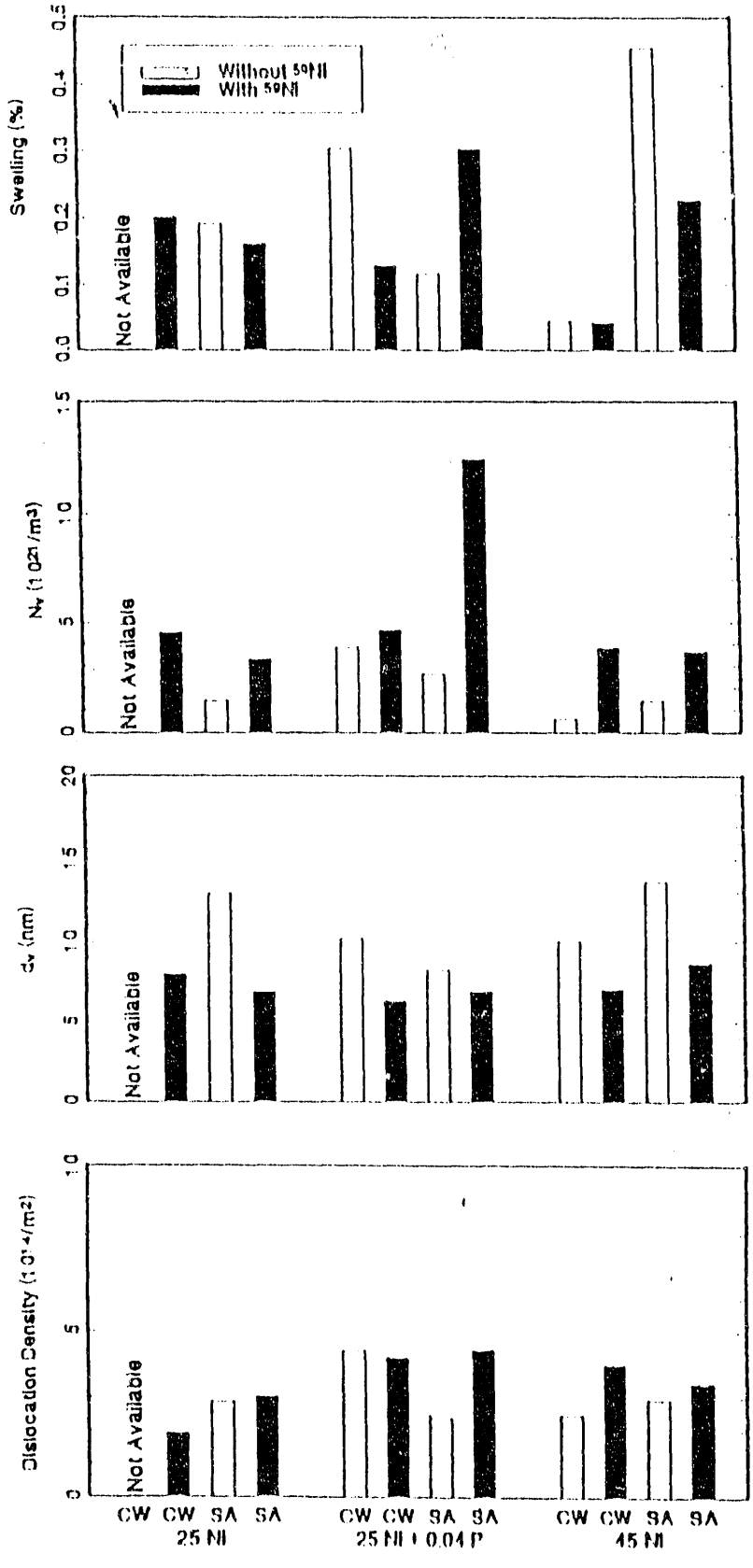

FIG. 8--Swelling, void number density, average void diameter, and total dislocation density measured in specimens irradiated at 365°C to 10.3 dpa, as a function of alloy composition and thermomechanical treatment.

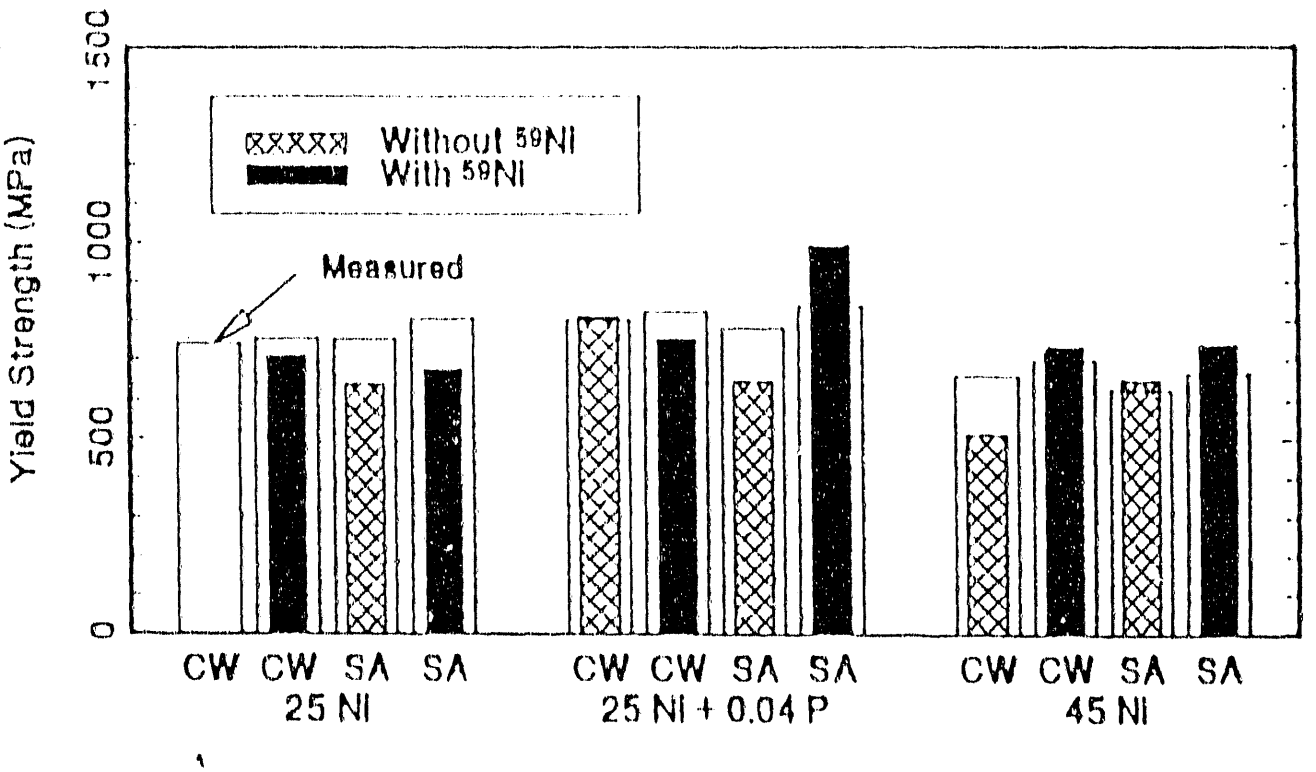

FIG. 9--A comparison of measured yield strength values (shown in outline) and those calculated from measured microstructural parameters for the three alloys irradiated to 10.3 dpa at 365°C (shown as shaded or solid bars).

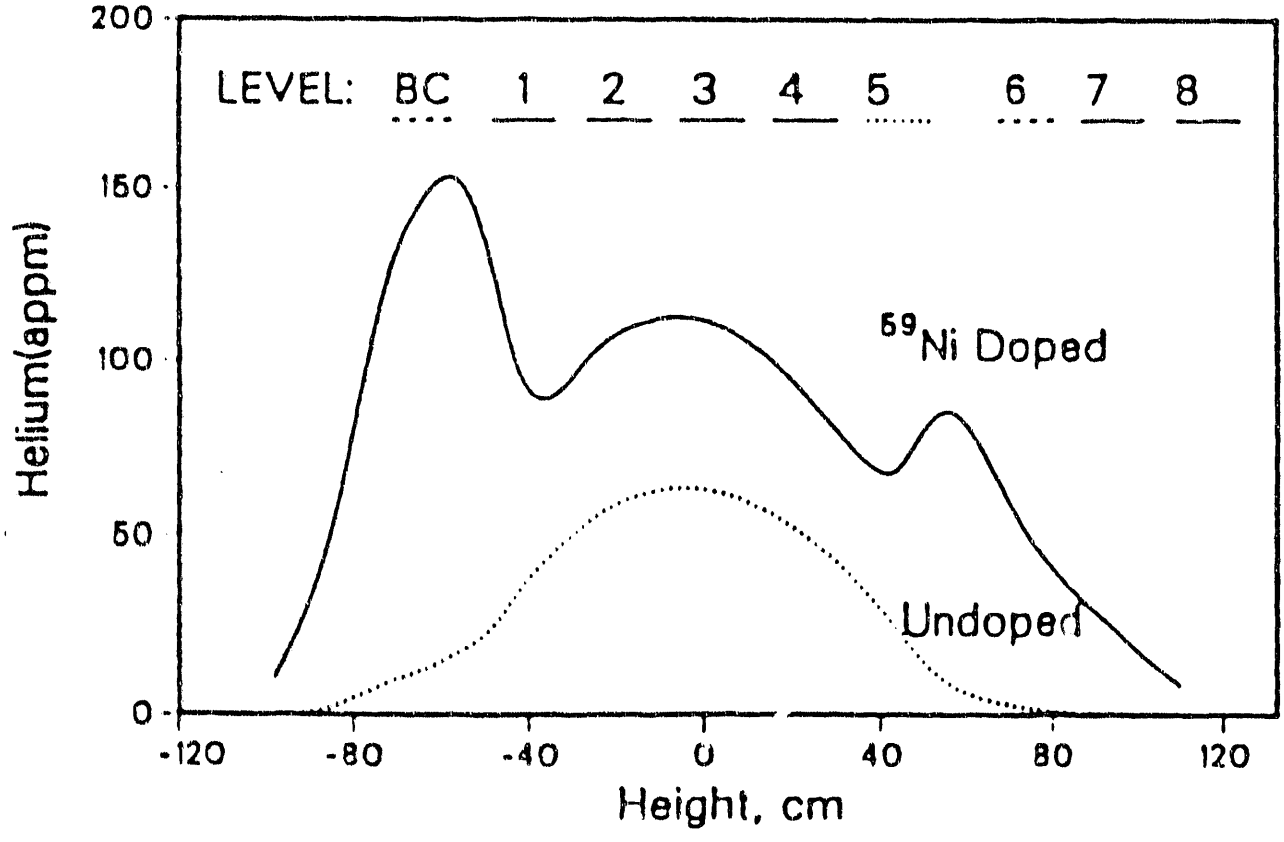

FIG. 10--Calculated helium production (appm) for both the ^{59}Ni-doped and undoped Fe-15Cr-45Ni alloy as a function of height in the MOTA assembly after the 1E and 1F irradiation.[6]

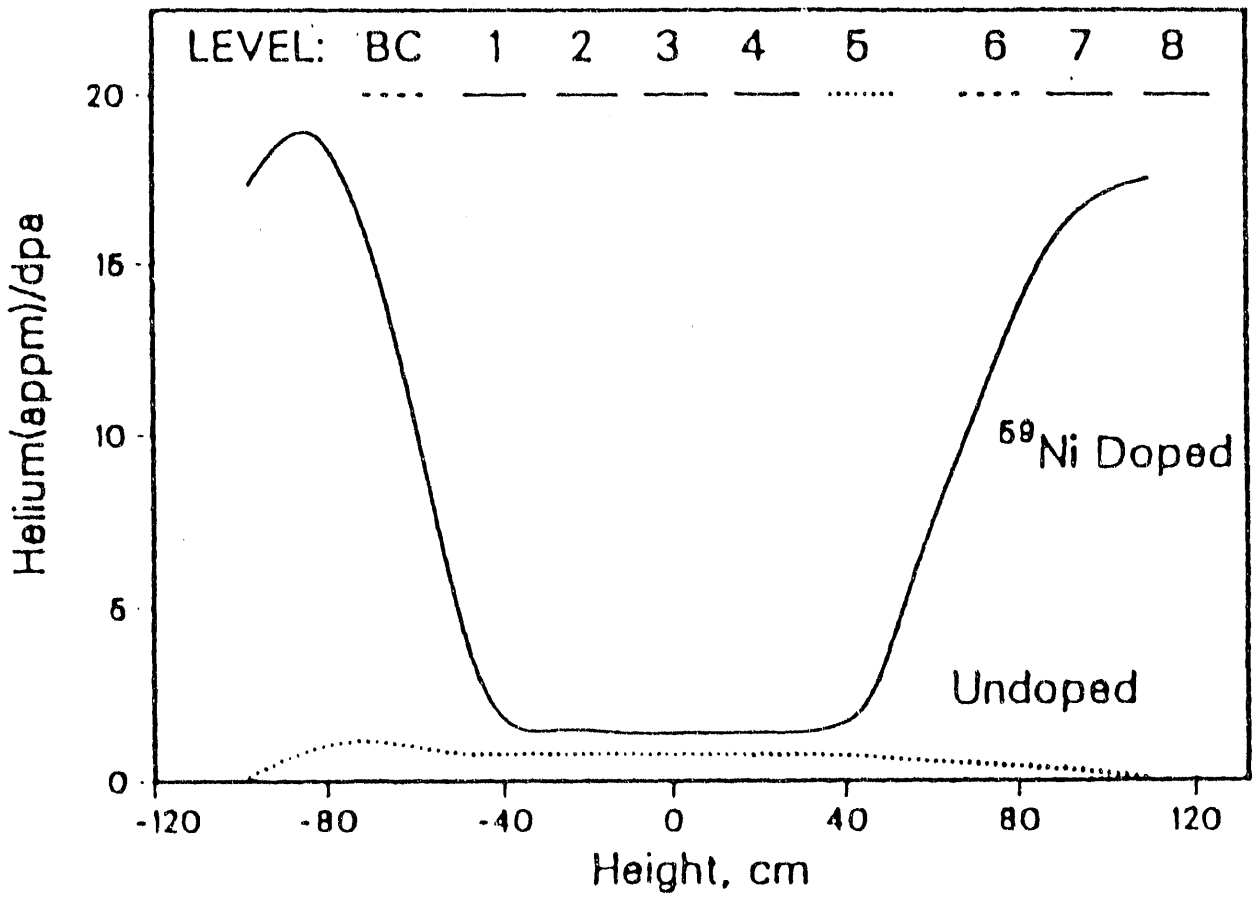

FIG. 11--Calculated helium (appm)-to-dpa ratios for both the ^{59}Ni-doped and undoped Fe-15Cr-45Ni alloy as a function of height in the MOTA assembly after the 1E and 1F irradiation.[6]

END

DATE
FILMED
9 / 28 / 92